Mathematical Sciences Technical Reports (MSTR)

Mathematics

12-5-2008

Electrothermal Imaging in One and Two Dimensions

Michael Janus

David Kibbling

Electrothermal Imaging in One and Two Dimensions

M. Janus and D. Kibbling

Adviser: Kurt M. Bryan

Mathematical Sciences Technical Report Series
MSTR 08-05

December 5, 2008

Electrothermal Imaging in One and Two Dimensions[1]

Michael Janus and David Kibbling

December 5, 2008

Contents

1 Introduction

Developing methods for the nondestructive testing of materials is an important area of research for industry. Situations often arise in which the integrity of an object is questioned, but testing it is very difficult. For example, a support bar may be embedded in a larger structure so that testing the bar's integrity directly would require the impractical task of breaking down the larger structure. Instead, the ends of the bar might be accessible without dismantling the enclosing structure. The goal of nondestructive testing is to use methods that require taking measurements at the ends of the bar alone to give information about the interior of the bar. Two approaches of recent interest for nondestructive testing involve thermal imaging (using temperature measurements) and impedance imaging (using electrical measurements).

This paper explores combining the two existing methods to produce a new method of performing nondestructive testing of materials. A one-dimensional bar and two-dimensional plate are considered. The basic idea behind this approach is as follows: suppose the interior of the object to be tested is corroded or damaged in some way. The corrosion will have an effect on the object's electrical properties; namely, its conductivity in the corroded region is changed. If current is injected into the object, it will produce heat due to Joule heating–just as current passing through any resistor produces heat. By observing the resulting temperature at the boundary of the object, the conductivity profile of the object can be reconstructed. This reconstructed profile contains information about the position and severity of the corrosion. The paper details the mathematics of such an approach and comments on its practicality. The technique has already been proven effective for locating interior cracks in an object; see [2, 3, 4].

1.1 The Forward Problem

Consider a domain $\Omega \subset \mathbb{R}^n$ whose boundary is $\partial\Omega$. Let $u(\vec{r})$ be the electric potential on Ω, $v(\vec{r}, t)$ be the temperature on Ω, and $\gamma(\vec{r})$ be the electrical conductivity on Ω, where $\vec{r}$ denotes the position vector in $\mathbb{R}^n$. We assume $0 < q_1 \leq \gamma(\vec{r}) \leq q_1 < \infty$ for some constants q_1, q_2. In the conventional electric conduction model (current flux equal to $-\gamma\nabla u$, plus conservation of charge inside Ω; note we assume current flows from higher to lower potential) the following equation is obeyed by u in Ω:

$$\nabla \cdot (\gamma\nabla u) = 0 \tag{1}$$

Equation (1) describes the flow of current throughout the domain Ω. This current generates Ohmic heating in the interior of Ω, with power density per unit area equal to $\gamma|\nabla u|^2$. Let us assume that the thermal conductivity and diffusivity of Ω is 1, for simplicity. Then a standard conservation of energy argument shows that the temperature $v(\vec{r}, t)$ obeys

$$v_t - \Delta v = \gamma|\nabla u|^2. \tag{2}$$

A simplifying assumption is implicit in the heat equation: the thermal conductivity is not considered affected by the corrosion. The term on the right side of equation (2) is the Joule heating term, which models the heat generated by current flowing through a resistor and couples equations (1) and (2).

The forward problem consists of knowing γ and then solving for $u(\vec{r})$ and $v(\vec{r}, t)$ on all of Ω, given certain boundary conditions for both functions on $\partial\Omega$ and an initial condition on v. This paper considers the case where the domain is thermally isolated, that is $\frac{\partial v}{\partial \mathbf{n}} = 0$ where $\mathbf{n}$ is the unit normal along the boundary. We also specify an input electrical flux in the form $\frac{\partial u}{\partial \mathbf{n}} = g$ on $\partial\Omega$ and an initial condition on v, typically $v(\vec{r}, 0) = 0$. The resulting forward problem is well-posed (possesses a unique solution, except that u is determined only up to an additive constant) and can be solved using numerical techniques. In our research the finite element software FEMLAB (now known as COSMOL Multiphysics) was used to solve these equations for a specified γ. The solutions to the forward problem help greatly in trying to solve the inverse problem which follows.

1.2 The Inverse Problem

The inverse problem consists of knowing the input electric current flux g on $\partial\Omega$ and the resulting response $v(\vec{r}, t)$ on part or all of $\partial\Omega$ over some time range, then trying to reconstruct $\gamma(\vec{r})$. We might also incorporate information concerning u on $\partial\Omega$. This inverse problem is not as well-known as the forward problem, so this research period was spent investigating it. The research process started by running the finite-element forward solver to solve equations (1) and (2) for a given γ, on both one- and two-dimensional regions Ω (typically the interval $(0, 1)$ or the square $(0, 1)^2$.) The values of $v(\vec{r}, t)$ on $\partial\Omega$ were then written to a data file. Based on the boundary data, attempts were made to reconstruct the original γ. These attempts and associated proven results are documented in the rest of the paper.

2 One Dimensional Case

2.1 Theory

In one dimension, the following theorem holds. Note that equations (1) and (2) make perfect sense in one-dimension.

Theorem 2.1 (One Dimensional Uniqueness Theorem)**:**
Let $\Omega = (0, 1)$. Suppose that $u(x)$ satisfies $(\gamma(x)u'(x))' = 0$ in Ω with the boundary conditions $-\gamma(0)u'(0) = -1$ and $\gamma(1)u'(1) = 1$ and $v(x, t)$ satisfies

$$v_t - v_{xx} = \gamma(x)(u'(x))^2, \ 0 < x < 1 \tag{3}$$
$$v_x(0, t) = v_x(1, t) = 0 \tag{4}$$
$$v(x, 0) = 0. \tag{5}$$

Then knowledge of $v(0, t)$ (or $v(1, t)$) for $0 < t < \infty$ uniquely determines the function $\gamma(x)$.

Proof. Note that $-\gamma(0)u'(0)$ is the input current flux at $x = 0$ and $\gamma(1)u'(1)$ is the input flux at $x = 1$; these are equal and of opposite sign, since the problem is steady-state (what goes in must come out at the same rate). We can write out the function $u(x)$ rather explicitly. From $(\gamma u')' = 0$ we may conclude that $\gamma u'(x)$ is constant and indeed from the boundary conditions

3

we have $\gamma(x)u'(x) = 1$. Thus $u'(x) = 1/\gamma(x)$. We also find (with the normalization $u(0) = 0$, since u is determined only up to an additive constant) that

$$u(x) = \int_0^x \frac{dz}{\gamma(z)}.$$

This means that

$$\gamma(u'(x))^2 = \frac{1}{\gamma(x)}. \tag{6}$$

We assume that v satisfies the insulating boundary conditions $v_x(0, t) = v_x(1, t) = 0$ for all t, and that $v(x, 0) = 0$. It is well-known that solutions to the heat equation under these conditions are unique. This can be shown with a simple energy argument; see [1]. We will demonstrate the existence of a solution via separation of variables and write the solution out rather explicitly. This is of value in solving the inverse problem.

Consider $v(x, t)$ of the form

$$v(x, t) = \sum_{j=0}^{\infty} c_j(t) \cos(j\pi x).$$

This function satisfies the boundary conditions $v_x(0, t) = v_x(1, t) = 0$. Let the jth Fourier coefficient of $\frac{1}{\gamma(x)}$ be denoted f_j. Then inserting v of the form hypothesized above into equation (3) implies

$$\sum_{j=0}^{\infty} (\dot{c}_j(t) + j^2\pi^2 c_j(t)) \cos(j\pi x) = \sum_{j=0}^{\infty} f_j \cos(j\pi x),$$

from which it follows that

$$\dot{c}_j(t) + j^2\pi^2 c_j(t) = f_j. \tag{7}$$

Solving this differential equation with the initial condition $v(x, 0) = 0$ (which implies $c_j(0) = 0$ for each j) gives

$$c_j(t) = \begin{cases} \frac{f_j}{j^2\pi^2}(1 - e^{-j^2\pi^2 t}), & \text{if } j \neq 0 \\ f_0 t, & \text{if } j = 0. \end{cases} \tag{8}$$

Using equation (8), the solution to the heat equation can be written as

$$v(x, t) = f_0 t + \sum_{j=1}^{\infty} \frac{f_j}{j^2\pi^2}(1 - e^{-j^2\pi^2 t}) \cos(j\pi x). \tag{9}$$

Then, on the boundary at $x = 0$,

$$v(0, t) = f_0 t + \sum_{j=1}^{\infty} \frac{f_j}{j^2\pi^2}(1 - e^{-j^2\pi^2 t}) = f_0 t + \sum_{j=1}^{\infty} \frac{f_j}{j^2\pi^2} - \sum_{j=1}^{\infty} \frac{f_j}{j^2\pi^2} e^{-j^2\pi^2 t} \tag{10}$$

4

From just this known boundary data at $x = 0$, the Fourier coefficients of $\frac{1}{\gamma(x)}$ can be recovered using an exponential stripping algorithm. The following succession of limits gives the values of the f_j's:

$$f_0 = \lim_{t \to \infty} \frac{v(0,t)}{t}$$

$$\sum_{j=1}^{\infty} \frac{f_j}{j^2 \pi^2} = \lim_{t \to \infty} v(0,t) - f_0 t$$

$$f_1 = -\pi^2 \lim_{t \to \infty} \frac{v(0,t) - f_0 t - \sum_{j=1}^{\infty} \frac{f_j}{j^2 \pi^2}}{e^{-\pi^2 t}}$$

$$f_2 = -4\pi^2 \lim_{t \to \infty} \frac{v(0,t) - f_0 t - \sum_{j=1}^{\infty} \frac{f_j}{j^2 \pi^2} + \frac{f_1}{\pi^2} e^{-\pi^2 t}}{e^{-4\pi^2 t}}$$

$$f_3 = -9\pi^2 \lim_{t \to \infty} \frac{v(0,t) - f_0 t - \sum_{j=1}^{\infty} \frac{f_j}{j^2 \pi^2} + \frac{f_1}{\pi^2} e^{-\pi^2 t} + \frac{f_2}{4\pi^2} e^{-4\pi^2 t}}{e^{-9\pi^2 t}}$$

$$f_4 = -16\pi^2 \lim_{t \to \infty} \frac{v(0,t) - f_0 t - \sum_{j=1}^{\infty} \frac{f_j}{j^2 \pi^2} + \frac{f_1}{\pi^2} e^{-\pi^2 t} + \frac{f_2}{4\pi^2} e^{-4\pi^2 t} + \frac{f_3}{3\pi^2} e^{-3\pi^2 t}}{e^{-16\pi^2 t}}$$

$$\vdots$$

Therefore, the Fourier coefficients of $\frac{1}{\gamma(x)}$ can be recovered using the just the data $v(0,t)$ for $0 < t < \infty$, and hence $\gamma(x)$ can be recovered uniquely. A similar argument shows that $\gamma(x)$ can be recovered from the data $v(1,t)$ for $0 < t < \infty$ as well. $\qquad \square$

Of course the proof of Theorem 2.1 also gives a constructive approach to recovering γ from data, which we illustrate in the next section.

2.2   Results

Theorem 2.1 illustrates that data taken at just one boundary is sufficient to recover the conductivity function of the bar—provided that data is taken for all time. Of course, in practice, data can only be taken for a finite time, thus making the precise computation of the limits described in the theorem impossible.

To solve the inverse problem computationally, an estimate of the function is made, by truncating the Fourier expansion,

$$v(0,t) \approx \tilde{v}(0,t) = f_0 t + \sum_{j=1}^{N} \frac{f_j}{j^2 \pi^2} (1 - e^{-j^2 \pi^2 t}) \tag{11}$$

$$= f_0 t + \sum_{j=1}^{N} \frac{f_j}{j^2 \pi^2} - \sum_{j=1}^{N} \frac{f_j}{j^2 \pi^2} e^{-j^2 \pi^2 t}, \tag{12}$$

for some $N \in \mathbb{N}$. With this estimation, a least square analysis can be performed to recover the f_j's. For example, if the temperature at $x = 0$ is taken every 0.001 seconds for $0 < t < 0.5$

(a total of 500 data points), the following quantity is minimized with respect to the unknown Fourier coefficients $f_0, \ldots, f_N$:

$$\sum_{k=1}^{500} (\tilde{v}(0, 0.005\,k) - v(0, 0.005\,k))^2 \tag{13}$$

This method can be improved by considering data on both ends of the bar. At the right boundary we have

$$v(1, t) \approx \tilde{v}(1, t) = f_0 t + \sum_{j=1}^{N} (-1)^j \frac{f_j}{j^2 \pi^2} (1 - e^{-j^2 \pi^2 t}) \tag{14}$$

$$= f_0 t + \sum_{j=1}^{N} (-1)^j \frac{f_j}{j^2 \pi^2} - \sum_{j=1}^{N} (-1)^j \frac{f_j}{j^2 \pi^2} e^{-j^2 \pi^2 t}. \tag{15}$$

Then the odd and even Fourier coefficients can be solved for separately, since

$$\tilde{v}(1, t) + \tilde{v}(0, t) = 2 f_0 t + \sum_{\substack{j>0 \text{ even}}}^{N} \frac{2 f_j}{j^2 \pi^2} - \sum_{\substack{j>0 \text{ even}}}^{N} \frac{2 f_j}{j^2 \pi^2} e^{-j^2 \pi^2 t}$$

$$\tilde{v}(1, t) - \tilde{v}(0, t) = - \sum_{\substack{j>0 \text{ odd}}}^{N} \frac{2 f_j}{j^2 \pi^2} + \sum_{\substack{j>0 \text{ odd}}}^{N} \frac{2 f_j}{j^2 \pi^2} e^{-j^2 \pi^2 t}.$$

As in equation (13), a least squares analysis can be performed to solve for the f_j's by minimizing

$$\sum_{k=1}^{500} [(\tilde{v}(1, 0.005\,k) + \tilde{v}(0, 0.005\,k)) - (v(1, 0.005\,k) + v(0, 0.005\,k))]^2 \tag{16}$$

and

$$\sum_{k=1}^{500} [(\tilde{v}(1, 0.005\,k) - \tilde{v}(0, 0.005\,k)) - (v(1, 0.005\,k) - v(0, 0.005\,k))]^2 \tag{17}$$

as functions of the f_j. The process is quite unstable, however, especially for the f_j in which j is large. This is illustrated below.

Example 2.2.1 (1D Reconstruction):

To test the algorithm for γ reconstruction outlined above, consider the function

$$\gamma(x) = \begin{cases} 60(x - 0.78)^2 + 0.3, & \text{if } 0.672 \leq x \leq 0.888 \\ 1, & \text{otherwise.} \end{cases} \tag{18}$$

The following graphs show the difference between the reconstructed 14-term Fourier approximation to the function (left) and its actual 14-term Fourier approximation (right).

6
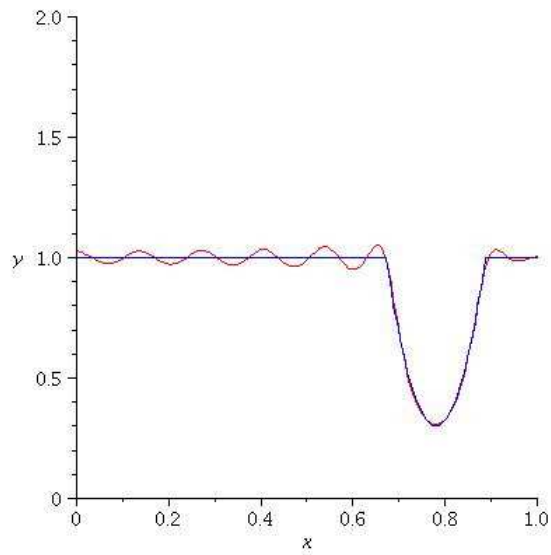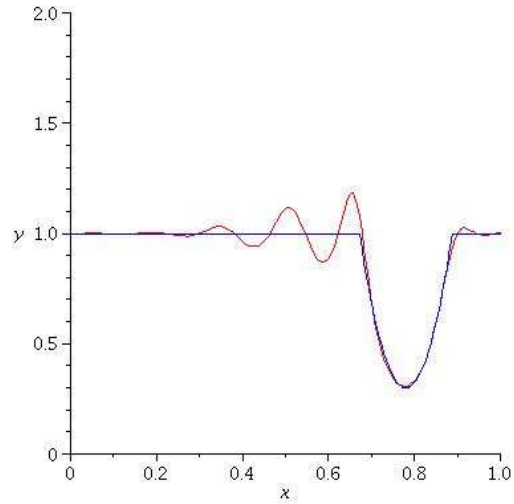
Example 2.2.1 illustrates how computational error affects the reconstruction process. This example reconstructed γ using a 14-term Fourier approximation. Adding higher order terms in this case introduces error that renders the reconstruction useless. The reason for the instability in the recovery of higher order terms can be seen in equation (8). The reconstruction algorithm solves for the $c_j(t)$'s from boundary data. In terms of the $c_j(t)$'s then, the f_j's are:

$$f_j = \frac{j^2\pi^2 c_j(t)}{1 - e^{\pi^2 j^2 t}} \tag{19}$$

Any error in the $c_j(t)$'s in the reconstruction gets magnified as j gets larger. This means the problem is particularly ill-posed. Generally, about 13 or 14 terms of the Fourier series of $\frac{1}{\gamma}$

7

can be reconstructed reasonably. The reconstruction is worse if the magnitudes of $\frac{1}{\gamma}$'s higher order Fourier coefficients are larger.

It would be worthwhile for a future REU group to pursue more effective methods for this exponential stripping algorithm.

2.3 Steady state theory

Some additional progress can be made by considering the steady-state version of the problem.

As noted in the proof of Theorem 2.1, $v(x)$ has the form

$$v(x) = f_0 t + \sum_{k=1}^{\infty} \frac{f_k}{k^2 \pi^2} \left(1 - e^{-k^2 \pi^2 t} \right) \cos(k\pi x).$$

We shall make the substitutions

$$w(x, t) = \sum_{k=1}^{\infty} \frac{f_k}{k^2 \pi^2} \left(1 - e^{-k^2 \pi^2 t} \right) \cos(k\pi x),$$

$$\widetilde{w}(x) = \lim_{t \to \infty} w(x, t) = \sum_{k=1}^{\infty} \frac{f_k}{k^2 \pi^2} \cos(k\pi x).$$

Then

$$v(x, t) = f_0 t + w(x, t) \sim f_0 t + \widetilde{w}(x). \tag{20}$$

To develop the steady state theory further, we let

$$\rho(x) = \frac{1}{\gamma(x)},$$

$$\rho^*(x) = \rho(x) - 1,$$

$$R_1^*(x) = \int_0^x \rho^*(z) \, dz, R_1^* = R_1^*(1),$$

$$R_2^*(x) = \int_0^x R_1^*(z) \, dz, R_2^* = R_2^*(1),$$

Note that ρ is the *resistivity* of the region. We then have $\rho = 1 + \rho^*$, so ρ^* is merely the perturbation of the corroded region from the nominal value of 1. Furthermore, let us define a *symmetric corroded region* to be an interval such that $\rho^*(x)$ (or ρ) is even with respect to some midpoint m. We may then state the following lemma.

Lemma 2.3.1:
If $\rho^*(x) \equiv 0$ except on a single symmetric corroded region (a, b), then $R_2^* = (1 - m)R_1^*$.

Proof. From the symmetry condition on ρ^* we may deduce the following symmetry relations, which are easily verified:

$$\rho^*(m+x) = \rho^*(m-x),$$
$$R_1^*(m+x) = R_1^* - R_1^*(m-x),$$
$$R_2^*(m+x) = R_2^*(m-x) + xR_1^*.$$

Since $\rho^*(x) \equiv 0$ for $x \leq a$, we find that $R_1^*(x) = R_2^*(x) = 0$ for all $x \leq a$. It follows from the symmetry relations that

$$R_1^*(b) = R_1^* - R_1^*(a) = R_1^*,$$
$$R_2^*(b) = R_2^*(a) + (b-m)R_1^* = (b-m)R_1^*.$$

From these statements we then find that

$$\begin{aligned}
R_2^* &= \int_0^1 R_1^*(x)\, dx \\
&= \int_0^b R_1^*(x)\, dx + \int_b^1 R_1^*(x)\, dx \\
&= R_2^*(b) + \int_b^1 R_1^*\, dx \\
&= (b-m)R_1^* + (1-b)R_1^* = (1-m)R_1^*.
\end{aligned}$$

$\square$

With this we establish the main result of this section:

Theorem 2.2 (Midpoint Formula)**:**
If $\rho^*(x) \equiv 0$ except on a single symmetric corroded region (a, b), then the midpoint m of this region is given as

$$m = \lim_{t \to \infty} \left(\frac{1}{2} + \frac{v(1,t) - v(0,t)}{u(1) - u(0) - 1} \right).$$

Proof. Since $(\gamma(x)u'(x))' = 0$ and $\gamma(0)u'(0) = 1$, it follows that $\gamma(x)u'(x) = 1$, and $u'(x) = \frac{1}{\gamma(x)} = \rho(x)$. Then

$$u(1) - u(0) = \int_0^1 \rho(x)\, dx = \int_0^1 (1 + \rho^*(x))\, dx = 1 + R_1^*.$$

For the heat equation $v_t - v_{xx} = \rho(x)$, the fact that $v_t - v_{xx} = f_0 + (w_t - w_{xx})$ and the approximation $w_t - w_{xx} \approx -\widetilde{w}''(x)$ we obtain $f_0 - \widetilde{w}''(x) = \rho(x)$ or

$$\widetilde{w}''(x) = f_0 - \rho(x)$$

where we make use of (20). Two integrations with respect to x then gives

$$\widetilde{w}'(x) - \widetilde{w}'(0) = f_0 x - R_1^*(x) - x, \tag{21}$$

$$\widetilde{w}(x) - \widetilde{w}(0) - \widetilde{w}'(0)x = \frac{1}{2}f_0 x^2 - R_2^*(x) - \frac{x^2}{2}. \tag{22}$$

Observe that since $v_x(x,t) = w_x(x,t) \sim \widetilde{w}'(x)$, the insulating boundary condition on $v(x,t)$ forces $\widetilde{w}'(0) = \widetilde{w}'(1) = 0$. Equation (21) in the case $x = 1$ then implies that $f_0 = 1 + R_1^*$. Applying Lemma 2.3.1 to (22) (and again note that $\widetilde{w}'(0) = 0$) in the case $x = 1$ produces

$$\begin{aligned}
\widetilde{w}(1) - \widetilde{w}(0) &= (1 + R_1^*)/2 - R_2^* - 1/2 \\
&= R_1^*/2 - (1 - m)R_1^* \\
&= (m - 1/2)R_1^*.
\end{aligned}$$

Solving for m and noting that

$$\lim_{t \to \infty} (v(1,t) - v(0,t)) = \widetilde{w}(1) - \widetilde{w}(0)$$

gives the desired formula

$$\begin{aligned}
m &= \frac{1}{2} + \frac{\widetilde{w}(1) - \widetilde{w}(0)}{R_1^*} \\
&= \lim_{t \to \infty} \left(\frac{1}{2} + \frac{v(1,t) - v(0,t)}{u(1) - u(0) - 1} \right).
\end{aligned}$$

$\square$

Note that the result $f_0 = 1 + R_1^*$ is independent of the assumptions on ρ, and is true in general.

3 Two Dimensional Case

3.1 Theory

In two dimensions, the following theorem holds:

Theorem 3.1 (Two Dimensional Partial Uniqueness Theorem)**:**
On the unit square $\Omega = (0,1)^2$, if $u(x,y)$ satisfies

$$\nabla \cdot (\gamma \nabla u) = 0 \quad on \ \Omega \tag{23}$$

$$\gamma \frac{\partial u}{\partial \mathbf{n}} = g \quad on \ \partial\Omega \tag{24}$$

$$\int_{\partial\Omega} u(x,y) \, dx = 0 \tag{25}$$

10

and

$$v_t - \Delta v = \gamma |\nabla u|^2 \quad in \ \Omega \tag{26}$$

$$\frac{\partial v}{\partial \mathbf{n}} = 0 \quad on \ \partial\Omega \tag{27}$$

$$v(x, y, 0) = 0, \tag{28}$$

then knowledge of $v(x, 0, t)$ for $0 < t < \infty$ uniquely determines the function $\gamma |\nabla u|^2$ on Ω.

Proof. Similar to Theorem 2.1, a standard separation of variables shows that the solution to the heat equation (26) with the boundary condition (27) has the form

$$v(x, y, t) = \sum_{j=0}^{\infty} \sum_{k=0}^{\infty} c_{jk}(t) \cos(j\pi x) \cos(k\pi y) \tag{29}$$

Let the Fourier coefficients of $\gamma |\nabla u|^2$ with respect to the orthogonal basis $\cos(j\pi x) \cos(k\pi y)$ be denoted f_{jk}. Then substituting v of the form in equation (29) into (26) implies

$$\dot{c}_{jk}(t) + (j^2 + k^2)\pi^2 c_{jk}(t) = f_{jk} \tag{30}$$

The solution to this differential equation is

$$c_{jk}(t) = \begin{cases} \frac{f_{jk}}{(j^2+k^2)\pi^2}(1 - e^{-(j^2+k^2)\pi^2 t}), & \text{if } j > 0 \text{ or } k > 0, \\ f_{00}t, & \text{if } j, k = 0. \end{cases} \tag{31}$$

Thus, in terms of the f_{jk}'s, the solution to the heat equation is

$$v(x, y, t) = f_{00}t + \underbrace{\sum_{j=0}^{\infty} \sum_{k=0}^{\infty}}_{j \neq 0 \text{ or } k \neq 0} \frac{f_{jk}}{(j^2 + k^2)\pi^2}(1 - e^{-(j^2+k^2)\pi^2 t}) \cos(j\pi x) \cos(k\pi y). \tag{32}$$

On the boundary $y = 0$,

$$v(x, 0, t) = f_{00}t + \underbrace{\sum_{j=0}^{\infty} \sum_{k=0}^{\infty}}_{j \neq 0 \text{ or } k \neq 0} \frac{f_{jk}}{(j^2 + k^2)\pi^2}(1 - e^{-(j^2+k^2)\pi^2 t}) \cos(j\pi x). \tag{33}$$

Now, fix a value for j. Exploiting Fourier's trick, it follows that if $j \neq 0$

$$2 \int_0^1 v(x, 0, t) \cos(j\pi x) \, dx = \sum_{k=0}^{\infty} \frac{f_{jk}}{(j^2 + k^2)\pi^2}(1 - e^{-(j^2+k^2)\pi^2 t}). \tag{34}$$

and if $j = 0$

$$\int_0^1 v(x, 0, t) \, dx = f_{00}t + \sum_{k=1}^{\infty} \frac{f_{0k}}{k^2\pi^2}(1 - e^{-k^2\pi^2 t}). \tag{35}$$

11

The integrals on the left side of equations (34) and (35) can be computed from the given boundary data. The f_{jk}'s can then be recovered from equations (34) and (35) using a similar exponential stripping process as outlined in Theorem 2.1. For example, the f_{2k}'s can be recovered as follows. For ease of notation, let

$$2 \int_0^1 v(x,0,t) \cos(2\pi x) \, dx = g(t).$$

Then,

$$g(t) = \sum_{k=0}^\infty \frac{f_{2k}}{(2^2+k^2)\pi^2} - \sum_{k=0}^\infty \frac{f_{2k}}{(2^2+k^2)\pi^2} e^{-(2^2+k^2)\pi^2 t}. \tag{36}$$

Computing the following limits gives the f_{2k}'s:

$$\sum_{k=0}^\infty \frac{f_{2k}}{(2^2+k^2)\pi^2} = \lim_{t\to\infty} \frac{g(t)}{t}$$

$$f_{20} = -4\pi^2 \lim_{t\to\infty} \frac{g(t) - \sum_{k=0}^\infty \frac{f_{2k}}{(2^2+k^2)\pi^2}}{e^{-4\pi^2 t}}$$

$$f_{21} = -5\pi^2 \lim_{t\to\infty} \frac{g(t) - \sum_{k=0}^\infty \frac{f_{2k}}{(2^2+k^2)\pi^2} + \frac{f_{20}}{4\pi^2}(e^{-4\pi^2 t})}{e^{-5\pi^2 t}}$$

$$f_{22} = -8\pi^2 \lim_{t\to\infty} \frac{g(t) - \sum_{k=0}^\infty \frac{f_{2k}}{(2^2+k^2)\pi^2} + \frac{f_{20}}{4\pi^2}(e^{-4\pi^2 t}) + \frac{f_{21}}{5\pi^2}(e^{-5\pi^2 t})}{e^{-8\pi^2 t}}$$

$$f_{23} = -13\pi^2 \lim_{t\to\infty} \frac{g(t) - \sum_{k=0}^\infty \frac{f_{2k}}{(2^2+k^2)\pi^2} + \frac{f_{20}}{4\pi^2}(e^{-4\pi^2 t}) + \frac{f_{21}}{5\pi^2}(e^{-5\pi^2 t}) + \frac{f_{22}}{8\pi^2}(e^{-8\pi^2 t})}{e^{-13\pi^2 t}}$$

$$\vdots$$

Therefore, the Fourier coefficients of $\gamma|\nabla u|^2$ can be recovered using the just the data $v(x,0,t)$ for $0 < t < \infty$, and hence $\gamma|\nabla u|^2$ can be recovered uniquely. $\qquad\square$

It should be clear that we can recover $\gamma|\nabla u|^2$ using the data for v from any side of the square Ω. Of course, the recovery of the Fourier coefficients is very ill-posed and, as in the one-dimensional case, it would be beneficial to explore more sophisticated and regularized algorithms than the least-square procedure we used. Also, the recovery of $\gamma|\nabla u|^2$ in Ω is only the first step in the recovery of γ. We will show how one might recover information about γ from knowledge of $\gamma|\nabla u|^2$ below, but first let us look at a specific example.

3.2 Results

As in the one-dimensional case, data can be collected for only a finite time. Thus, the exponential stripping method of recovering the Fourier coefficients must be abandoned in practice. In equations (34) and (35), each infinite series must again be truncated at some $N_j \in \mathbb{N}$. Then, data can be taken at N_j different times, generating N_j linear equations for the N_j unknown Fourier coefficients. As j grows larger, fewer Fourier terms can be solved for reliably, so picking the N_j's differs for every j to be solved.

Example 3.2.1 (2D Reconstruction)**:**

The table below illustrates a function for $\gamma|\nabla u|^2$ that has only low order coefficients. The vertical values are the j values, while the horizontal values are the k values.

f_{jk}	0	1	2	3	4	5	6	7	8
0	2.12	0.00	0.00	0.00	0.00	0.00	0.00	0.00	0.00
1	0.00	1.54	1.23	0.00	0.65	1.87	2.13	0.00	0.12
2	0.00	1.45	0.00	0.56	2.43	0.00	0.00	0.00	0.00
3	0.99	0.00	2.06	1.18	0.00	0.37	1.32	0.00	0.00
4	1.93	1.12	0.00	0.78	0.00	0.00	0.00	0.00	0.00
5	0.00	2.04	1.20	0.00	0.00	0.00	0.00	0.00	0.00
6	0.94	0.00	1.60	0.00	0.00	0.00	0.00	0.00	0.00
7	0.00	2.81	0.39	1.83	0.00	0.00	0.00	0.00	0.00

The graph of the function follows:
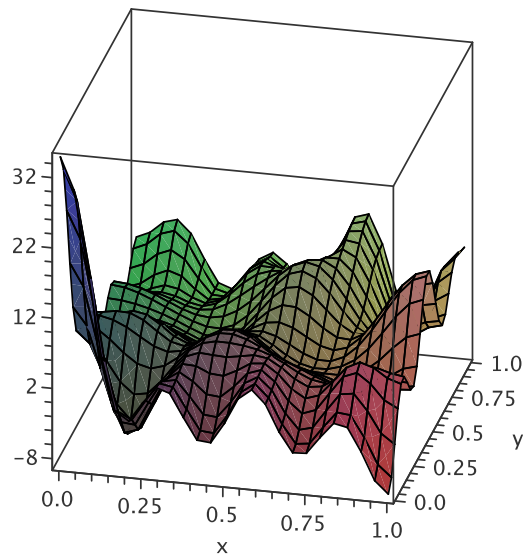
The following table shows the reconstructed f_{jk} from the boundary data for v. The function v was computed numerically using FEMLAB.

13

f_{jk}	0	1	2	3	4	5	6	7	8
0	2.123	0.000	0.000	0.000	0.000	0.000	0.000	0.000	0.000
1	0.000	1.542	1.232	0.000	0.651	1.872	2.135	0.002	0.121
2	0.000	1.452	0.000	0.560	2.435	0.003	0.004	0.005	0.002
3	0.992	0.001	2.064	1.180	0.002	0.368	1.323	0.001	0.000
4	1.935	1.117	0.005	0.776	0.004	0.002	0.001	0.000	0.000
5	0.002	2.047	1.197	0.005	0.005	0.001	0.000	0.000	0.000
6	0.938	0.006	1.598	0.002	0.000	0.000	0.000	0.000	0.000
7	0.004	2.807	0.394	1.831	0.000	0.000	0.000	0.000	0.000

Once again, when only low order Fourier coefficients are present, the reconstruction algorithm works quite well. However, the more Fourier coefficients present in $\gamma|\nabla u|^2$, the worse the reconstruction algorithm works. The ill-posedness of the problem is evident, just as it was in one-dimension. Considering equation (31) and solving for f_{jk} gives

$$f_{jk} = \frac{(j^2 + k^2)\pi^2 c_{jk}(t)}{1 - e^{\pi^2(j^2+k^2)t}} \tag{37}$$

Any error in the reconstruction of the $c_{jk}(t)$'s gets multiplied greatly as j and k increase. Only the upper left corner of the f_{jk} matrix can be solved for reasonably, and non-negligible higher order Fourier coefficients of $\gamma|\nabla u|^2$ make the reconstruction worse.

3.3   Linearization

We have been unable to develop an algorithm for recovering γ from knowledge of $\gamma|\nabla u|^2$, or indeed, even to prove that knowledge of $\gamma|\nabla u|^2$ uniquely determines γ in the most general setting. However, we have made progress in analyzing a linearized version of the problem, which we detail below.

Let $\gamma = 1 + \delta(x, y)$, $u = u_0 + \epsilon(x, y)$, and $f = \gamma|\nabla u|^2 = |\nabla u_0|^2 + h$, where $u_0(x, y)$ satisfies Laplace's equation with Neumann data g. We will consider γ to be a small perturbation of the constant conductivity 1 (that is, δ should be small, say in supremum norm), so the solution u should be a small perturbation of u_0. If we insert γ and u of this form into equations (23)-(24) and drop all terms higher than first order we obtain

$$
\begin{aligned}
\nabla \cdot (\gamma \nabla u) &= \gamma \Delta u + \nabla \gamma \cdot \nabla u \\
&= (1 + \delta)\Delta(u_0 + \epsilon) + \nabla(1 + \delta) \cdot \nabla(u_0 + \epsilon) \\
&= \Delta\epsilon + \nabla\delta \cdot \nabla u_0 + \text{ quadratic terms} \\
&= 0 \text{ in } \Omega
\end{aligned}
$$

for the PDE, while the boundary condition yields

$$
\begin{aligned}
\gamma\frac{\partial u}{\partial \mathbf{n}} &= (1 + \delta)\frac{\partial(u_0 + \epsilon)}{\partial \mathbf{n}} = g + \delta g + \frac{\partial\epsilon}{\partial \mathbf{n}} + \text{ quadratic terms} \\
&= g \text{ on } \partial\Omega
\end{aligned}
$$

14

and the approximation to f yields

$$\begin{aligned}
f &= \gamma|\nabla u|^2 \text{ in } \Omega \\
&= (1+\delta)(|\nabla u_0|^2 + 2\nabla u_0 \cdot \epsilon + |\nabla \epsilon|^2) \\
&= |\nabla u_0|^2 + \delta|\nabla u_0|^2 + 2\nabla u_0 \cdot \nabla \epsilon + \text{ quadratic terms.} \\
&= |\nabla u_0|^2 + h.
\end{aligned}$$

Dropping the (formally) small quadratic terms and simplifying these results leads to the following problem in which the relation between ϵ and δ has been linearized,

$$\Delta \epsilon = -\nabla u_0 \cdot \nabla \delta \text{ in } \Omega \tag{38}$$

$$\frac{\partial \epsilon}{\partial \mathbf{n}} = -\delta g \text{ on } \partial \Omega \tag{39}$$

$$\delta|\nabla u_0|^2 + 2\nabla u_0 \cdot \nabla \epsilon = h \text{ in } \Omega \tag{40}$$

We also assume that u_0 shares the zero line integral condition (25) of u, so that

$$\int_{\partial \Omega} \epsilon(x,y)\, ds = \int_{\partial \Omega} u(x,y)\, ds - \int_{\partial \Omega} u_0(x,y)\, ds = 0. \tag{41}$$

For the linearized forward problem we consider ϵ as the unknown, δ, g, and h as given (note u_0 is determine by g). The corresponding inverse problem is to determine δ from knowledge of ϵ, g and h.

We shall restrict our attention to the special case where $\Omega = (0,1)^2$, $\delta \equiv 0$ on $\partial \Omega$, and g is chosen such that $u_0(x,y) = x$ in Ω (thus g corresponds to input flux -1 on the left, 1 on the right, zero at the top and bottom of Ω.) The condition $\delta = 0$ on $\partial \Omega$ models the case in which the interior damage lies strictly away from the boundary. Equations (38)-(40) then become

$$\Delta \epsilon = -\frac{\partial \delta}{\partial x} \text{ in } \Omega \tag{42}$$

$$\frac{\partial \epsilon}{\partial \mathbf{n}} = -\delta g \text{ on } \partial \Omega \tag{43}$$

$$\delta + 2\frac{\partial \epsilon}{\partial x} = h \text{ in } \Omega. \tag{44}$$

If we use (44) to solve for δ and insert this into (42) we find that ϵ satisfies

$$\frac{\partial^2 \epsilon}{\partial y^2} - \frac{\partial^2 \epsilon}{\partial x^2} = -\frac{\partial h}{\partial x} \tag{45}$$

in Ω. Additionally, since δ vanishes on $\partial \Omega$, from (42) we find that $\frac{\partial \epsilon}{\partial \mathbf{n}}$ must also vanish on $\partial \Omega$. We may now state a uniqueness theorem for equations (42)-(44).

Theorem 3.2 (Uniqueness Theorem for the Linearized Problem)**:**
Let g be chosen such that $u_0(x) = x$ in $\Omega = (0,1)^2$ and suppose $\delta \equiv 0$ on $\partial \Omega$. Then knowledge of h in Ω uniquely determines ϵ and δ in Ω.

Proof. We shall demonstrate that if h vanishes everywhere in Ω then ϵ and δ vanish everywhere. The linearity of ϵ and δ in (42)-(44) then implies that any solution to the linearized problem must be unique. Note that since δ vanishes on $\partial\Omega$, from the assumption $h \equiv 0$ we see from equation (43) that ϵ_x must also vanish on $\partial\Omega$ (at least if ϵ is sufficiently smooth).

Let $\mathcal{E}(y)$ denote the 'energy integral'

$$\mathcal{E}(y) = \frac{1}{2}\int_0^1 \left(\epsilon_x^2(x,y) + \epsilon_y^2(x,y)\right)\,dx.$$

Since $h \equiv 0$ equation (45) forces

$$\begin{aligned}
\mathcal{E}'(y) &= \int_0^1 (\epsilon_x \epsilon_{xy} + \epsilon_y \epsilon_{yy})\,dx \\
&= \int_0^1 (\epsilon_x(\epsilon_{yx}) + \epsilon_y(\epsilon_{xx}))\,dx \\
&= \int_0^1 (\epsilon_x \epsilon_y)_x\,dx \\
&= \epsilon_x \epsilon_y \Big|_{x=0}^{x=1} = 0,
\end{aligned}$$

since $\epsilon_x = \pm\frac{\partial\epsilon}{\partial\mathbf{n}}$ vanishes for $x = 0$ and $x = 1$. Thus $\mathcal{E}(y)$ is constant. Additionally,

$$\mathcal{E}(0) = \frac{1}{2}\int_0^1 (\epsilon_x(x,0)^2 + \epsilon_y(x,0)^2)\,dx = 0$$

since ϵ_x and ϵ_y vanish for $y = 0$. Thus both partial derivatives of ϵ must vanish everywhere and $\epsilon(x,y)$ must be a constant. Equation (41) then forces $\epsilon(x,y) \equiv 0$ and $\delta(x,y) = -2\epsilon_x \equiv 0$. $\qquad\square$

It's worth noting that uniqueness may fail without the assumption the $\delta \equiv 0$ on $\partial\Omega$. Consider, for example,

$$\epsilon(x,y) = \cos(\pi x)\cos(\pi y)$$

with

$$\delta = -2\epsilon_x = 2\pi\sin(\pi x)\cos(\pi y).$$

It's easy to check that (with $h = 0$ and g as above) these choices satisfy equations (42)-(44).

3.4 Reconstruction in the Linearized Problem

We again consider the special case from above, in which g is chosen so that $u_0(x,y) = x$, and assume $\delta \equiv 0$ on $\partial\Omega$. In this case the solution to (42)-(43) can be written out via a Fourier expansion (note (43) is just $\frac{\partial\epsilon}{\partial\mathbf{n}} = 0$) and is in fact

$$\epsilon(x,y) = -\frac{1}{\pi^2}\sum_{j,k\geq 0}\frac{q_{jk}}{j^2+k^2}\cos(j\pi x)\cos(k\pi y) \tag{46}$$

16

where $q_{00} = 0$ (since $-\delta_x$ must integrate to zero over Ω if $\frac{\partial \epsilon}{\partial \mathbf{n}} \equiv 0$) and

$$
q_{j0} = -2 \int_0^1 \int_0^1 \delta_x(x,y) \cos(j\pi x)\, dx\, dy = -2j\pi \int_0^1 \int_0^1 \delta(x,y) \sin(j\pi x)\, dx\, dy
$$

$$
q_{0k} = -2 \int_0^1 \int_0^1 \delta_x(x,y) \cos(k\pi y)\, dx\, dy = 0
$$

$$
q_{jk} = -4 \int_0^1 \int_0^1 \delta_x(x,y) \cos(j\pi x)\cos(k\pi y)\, dx\, dy = -4j\pi \int_0^1 \int_0^1 \delta(x,y) \sin(j\pi x)\cos(k\pi y)\, dx\, dy
$$

all follow from integration by parts. The q_{jk} are of course the Fourier cosine coefficients for $-\delta_x$, that is,

$$
-\delta_x(x,y) = \sum_{j,k \geq 0} q_{jk} \cos(j\pi x)\cos(k\pi y)
$$

from which we find (integrate in x and use $\delta = 0$ on the boundary)

$$
\delta(x,y) = - \sum_{j>0,k\geq 0} \frac{q_{jk}}{j\pi} \sin(j\pi x)\cos(k\pi y) \tag{47}
$$

With (46) in hand we can use (44). In particular, expand $h(x,y)$ into a Fourier sine/cosine series, as

$$
h(x,y) = \sum_{j>0,k\geq 0} h_{jk} \sin(j\pi x)\cos(k\pi y)
$$

where as usual (note $j > 0$, while $k \geq 0$, so h_{j0} is a special case)

$$
h_{j0} = 2 \int_0^1 \int_0^1 h(x,y) \sin(j\pi x)\, dx\, dy
$$

$$
h_{jk} = 4 \int_0^1 \int_0^1 h(x,y) \sin(j\pi x)\cos(k\pi y)\, dx\, dy.
$$

Equation (44) becomes, after matching like coefficients,

$$
-\frac{q_{jk}}{j\pi} + 2\frac{j}{\pi}\frac{q_{jk}}{j^2 + k^2} = h_{jk}
$$

or after simplifying

$$
\frac{(j^2 - k^2)q_{jk}}{j\pi(j^2 + k^2)} = h_{jk}. \tag{48}
$$

We can solve for q_{jk} as

$$
q_{jk} = j\pi \frac{j^2 + k^2}{j^2 - k^2} h_{jk}, \tag{49}
$$

at least if $j \neq k$. The case $j = k$ is dealt with below.

In short, once we know the h_{jk} we can solve for the q_{jk} and then use (47) to reconstruct. The Fourier $\sin(j\pi x)\cos(k\pi y)$ coefficients for δ are then given by

$$
\delta_{jk} = -\frac{j^2 + k^2}{j^2 - k^2} h_{jk}. \tag{50}
$$

17

From equation (48) it seems that the function h does not encode all of the information necessary to recover q, since $h_{jj} = 0$ for all j regardless of the value of q_{jj}. Thus uniqueness may not hold for the linearized problem. Nonetheless, we can recover the off-diagonal coefficients. This is an issue that needs further exploration, perhaps by next year's REU group.

4   Further Work

Ideas: Better, stabler procedures for exponential stripping. Reconstruction of diagonal coefficients (more generally, reconstruction for the linearized 2D problem), and generalization of 2D reconstruction and uniqueness to other input fluxes for g, more general domains, 3D. Also, computational examples that put the whole thing together (recover $\gamma|\nabla u|^2$ from thermal data, then use linearized reconstruction to get γ). Also, explore the full nonlinear problem in 2D. Apply to more specific types of damage, e.g., cracks. Add in possibility that thermal properties change too.

References

[1] W. Strauss, *Partial Differential Equations: An Introduction,*, John Wiley and Sons, Inc., 1992.

[2] T. Sakagami and S. Kubo, "Development of a New Crack Identification Technique Based on Near-Tip Singular Electrothermal Field Measured by Lock-in Infrared Thermography", JSME International Journal, Vol. 44, No. 4, 2001, pp. 528-534.

[3] G. Zenzinger, J. Bamberg, W. Satzger, and V. Carl, "Thermographic Crack Detection by Eddy Current Excitation," Nondestructive Testing and Evaluation, Vol. 22, Issues 2 and 3, 2007, pp. 101-111.

[4] B. Oswald-Tranta, "Thermo-Inductive Crack Detection," Nondestructive Testing and Evaluation, Vol. 22, Issues 2 and 3, 2007, pp. 137-153.